Supplemental Information

Increased ACTL6A Occupancy Within mSWI/SNF Chromatin Remodelers Drives Human Squamous Cell Carcinoma

Chiung-Ying Chang, Zohar Shipony, Sherry G. Lin, Ann Kuo, Xiaochen Xiong, Kyle M. Loh, William J. Greenleaf, Gerald R. Crabtree

SUPPLEMENTAL FIGURES

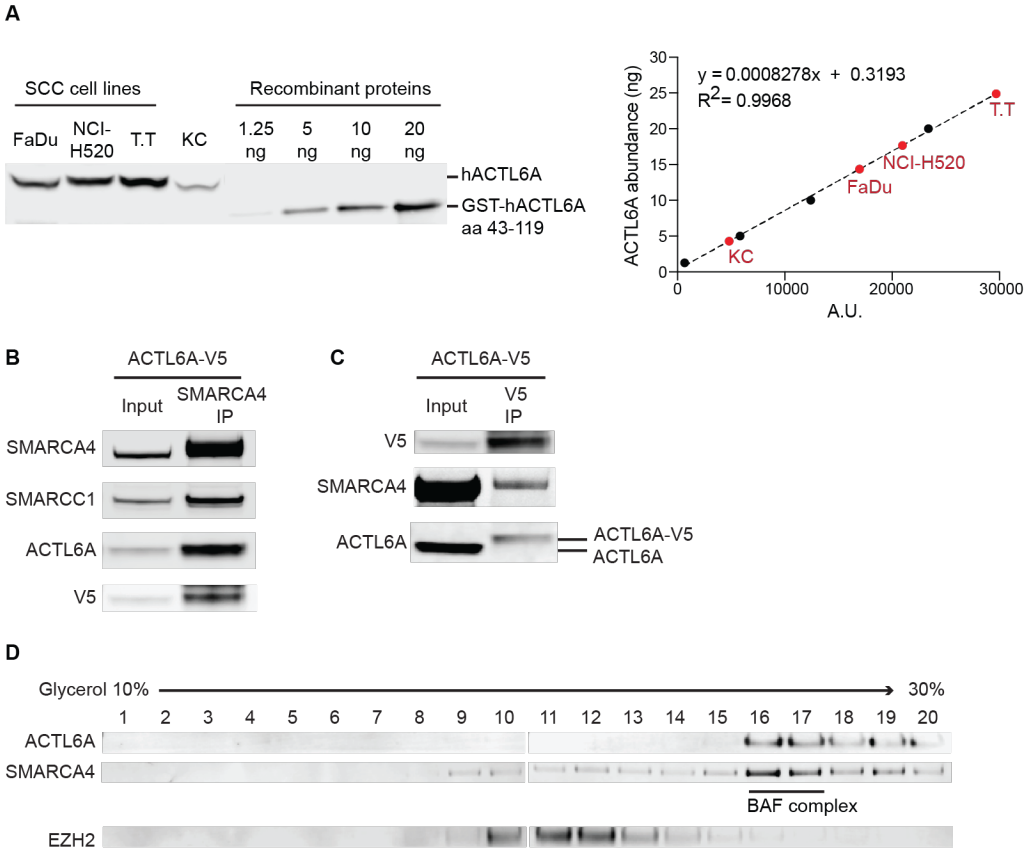

Figure S1. *ACTL6A* overexpression does not induce its dimerization and most of ACTL6A proteins associate with BAF complexes in SCC cells. Related to Figure 2.
(A) Left: Western blots for whole cell lysates from 300,000 cells of indicated cell lines and ACTL6A recombinant proteins. SCC cell lines: FaDu (head-and-neck), NCI-H520 (lung), and T.T (esophageal). KC: primary normal human keratinocytes. Right: Quantifications for Western blots. A.U.: arbitrary unit of Western blot integrated intensity. Linear regression line was generated from serially diluted ACTL6A recombinant proteins (black circles) and used for calculating ACTL6A abundance (ng) in cells (red circles). (B) Co-IP by SMARCA4 antibody using nuclear extracts from FaDu SCC cells infected with lentivirus expressing C-terminal V5-tagged ACTL6A. Note the incorporation of ACTL6A-V5 into BAF complexes as endogenous ACTL6A. (C) Co-IP by V5 antibody as (B). Note endogenous ACTL6A does not bind V5-tagged ACTL6A. (D) Density sedimentation and immunoblots for nuclear extracts from SCC cells. Note ACTL6A co-migrated with SMARCA4 marking BAF complexes in high molecular mass fractions 16-17 as a full complex. EZH2: subunit of PRC2 complexes as a control.

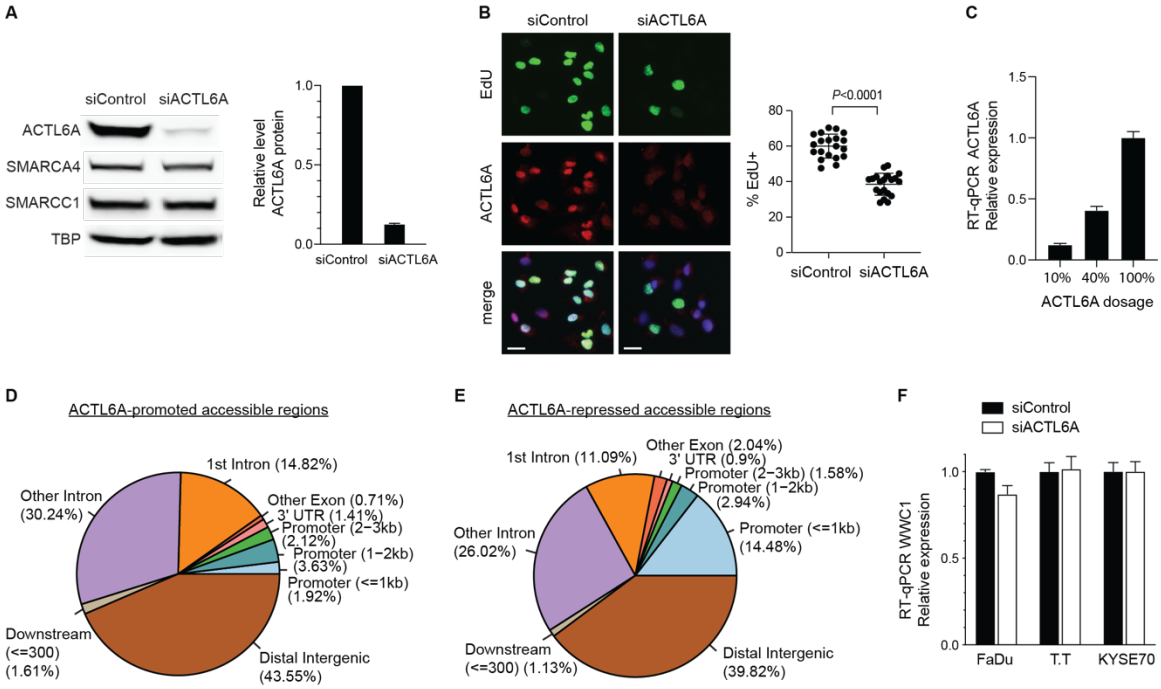

Figure S2. ATAC-seq analyses identify accessible chromatin regions regulated by ACTL6A in SCC cells. Related to Figure 3.

(A) Western blots for cell lysates from FaDu SCC cells 72h after transfection with *ACTL6A* siRNA (siACTL6A) or control siRNA (siControl). Quantifications of ACTL6A protein levels in siACTL6A relative to siControl cells. TBP: TATA-box-binding protein as loading control. (B) Immunostaining showing decreased SCC cell proliferation in response to *ACTL6A* knockdown. Assessment by the incorporation of EdU (5-ethynyl-2'-deoxyuridine) applied 1.5h before analysis, 72 hours after siRNA transfection. Quantifications: % of EdU+ cells. Scale bars: 20 μm. Mean ± SEM. (C) RT-qPCR showing ACTL6A intermediate- and high- level knockdown conditions upon different *ACTL6A* siRNA doses (40% or 10% remaining *ACTL6A*) relative to siControl (100%) used in Figure 3B and 3C. Mean ± SEM. (D) Annotation pie chart of regions with decreased accessibility by siACTL6A compared to siControl in FaDu SCC cells from ATAC-seq analysis. (E) As in (D) for regions with increased accessibility by siACTL6A compared to siControl. (F) Transcription factor (TF) motif enrichment within regions with increased accessibility in siACTL6A versus siControl FaDu cells. Matches: number of peaks containing matched TF binding motifs. (F) RT-qPCR showed no significant changes in *WWC1* expression levels 72 hours after siACTL6A transfection compared to siControl in three SCC cell lines. Mean ± SEM. **P* < 0.05.

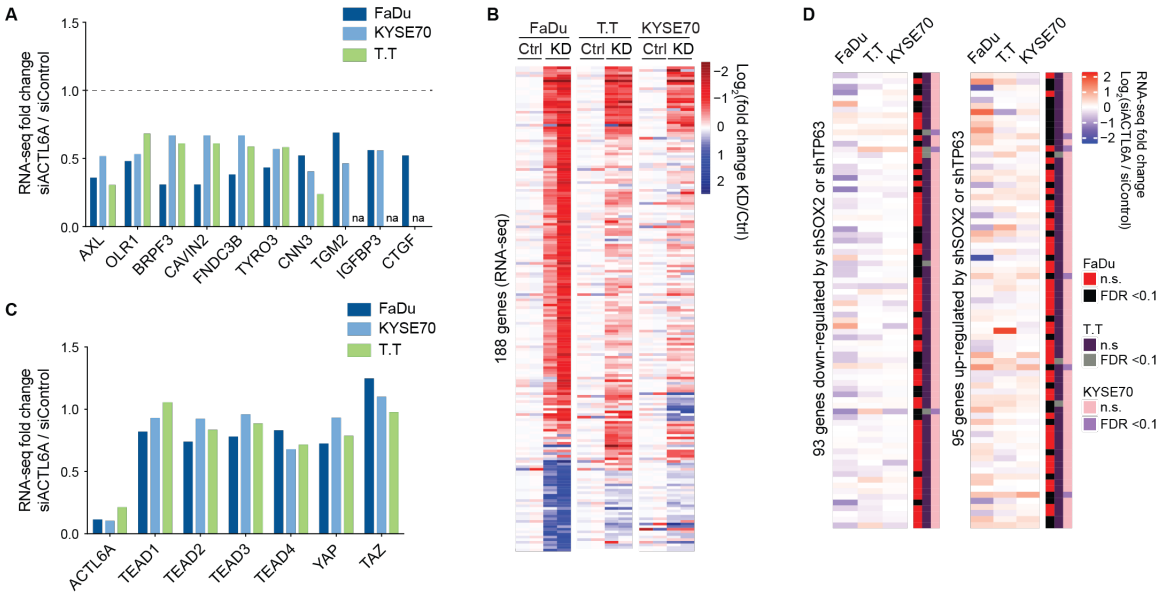

Figure S3. Transcriptome analyses by RNA-seq reveal ACTL6A regulates the expression of YAP target genes and a distinct set of genes from SOX2 and TP63. Related to Figure 3. (A) Relative expression levels of YAP target genes from RNA-seq analyses between siACTL6A siControl in three SCC cell lines. na: not available (not expressed). (B) Hierarchical clustering of RNA-seq analyses showing 188 genes with differential expression between siACTL6A (KD) and siControl (Ctrl) in at least two of three SCC cell lines. FDR < 0.05. (C) Relative expression levels of *YAP*, *TAZ*, *TEAD1-4* from RNA-seq analyses in siACTL6A cells normalized to siControl values. (D) Heat maps showing the RNA level fold-changes between siACTL6A versus siControl in three SCC cell lines across SOX2 and TP63 co-regulated genes. *SOX2* shRNA (shSOX2) or *TP63* shRNA (shTP63) knockdown experiments (Watanabe et al., 2014) were done in KYSE70 SCC cell line. Binary code on the right: FDR< 0.1 or not significant (n.s.).

A

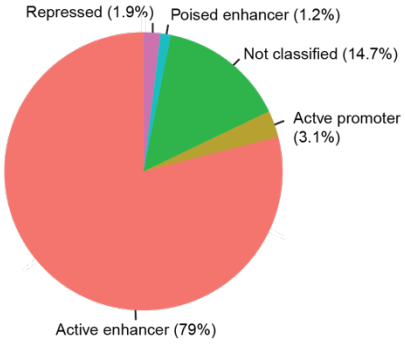

B

6,251 joint peaks between YAP, TEAD1 and SMARCC1 CUT&RUN

Rank	Motif	P-value	% of Targets	Best Match
1		$1x10^{-1146}$	64.49%	TEAD4 (TEA)
2		$1x10^{-265}$	55.22%	Fos (bZIP)
3		$1x10^{-58}$	28.08%	NEUROG2
4		$1x10^{-39}$	11.45%	POL009.1_DCE_S_II
5		$1x10^{-30}$	14.33%	TFAP2E

C

40,551 peaks from SMARCC1 CUT&RUN

Rank	Motif	P-value	% of Targets	Best Match
1		$1x10^{-5642}$	56.09%	FOSL2::JUNB
2		$1x10^{-444}$	6.79%	Sp2(Zf)
3		$1x10^{-126}$	20.94%	TEAD(TEA)
4		$1x10^{-123}$	6.59%	NFY(CCAAT)
5		$1x10^{-112}$	46.26%	TFAP2A

D

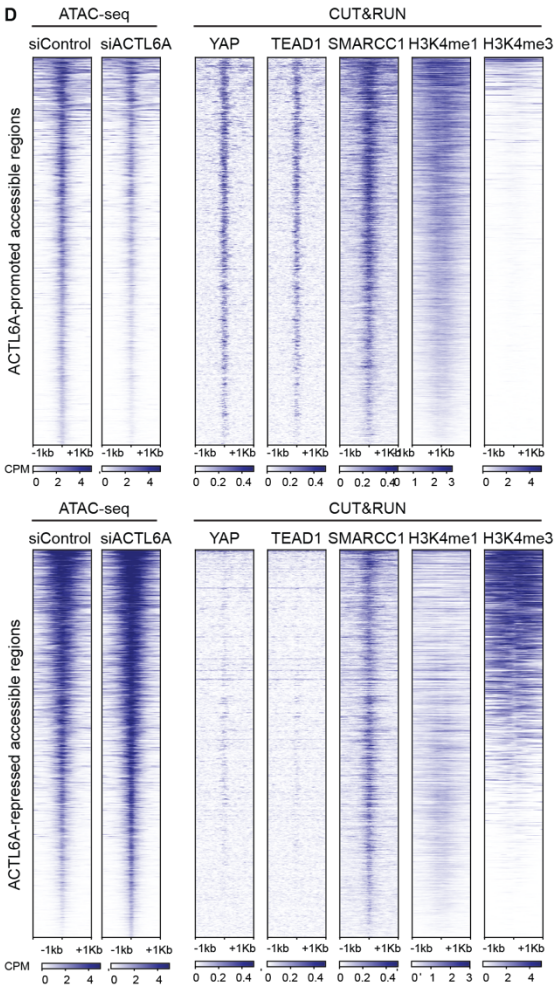

E

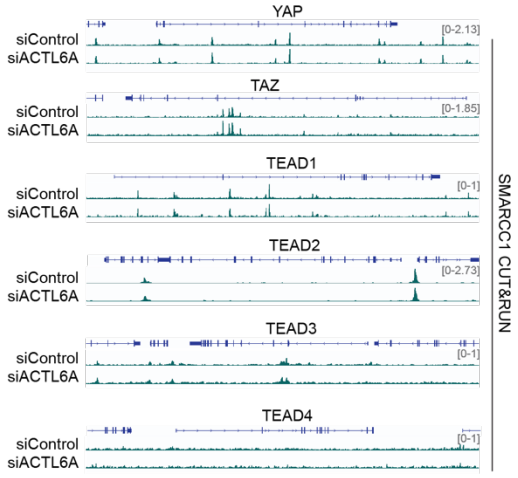

F

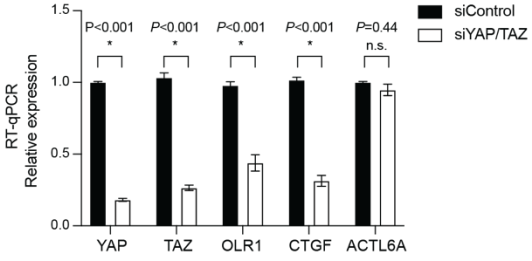

Figure S4. CUT&RUN profiling reveals the co-localization of YAP, TEAD1 and BAF complexes on chromatin in SCC cells. Related to Figure 4.
(A) Distribution of YAP, TEAD1 and BAF-subunit SMARCC1 co-occupied regions identified by CUT&RUN in FaDu SCC cells. Classification is based on the presence of histone marks identified by CUT&RUN: active enhancers- H3K27Ac^{+} H3K4me1^{+} (79 %); poised enhancers- H3K4me1^{+} H3K27me3^{+} (1.2 %); active promoters- H3K4me3+ H3K27me3^{-} (3.1 %); poised promoter- H3K4me3+ H3K27me3^{+} (0 %); repressed- H3K27me3^{+}(1.9 %). (B) *De novo* motif analysis by HOMER for regions co-bound by YAP, TEAD1 and SMARCC1 identified by CUT&RUN. (C) As in (B), for regions bound by SMARCC1. (D) Heat maps for ATAC-seq and indicated CUT&RUN profiles around regions with decreased accessibility (top) and increased accessibility (bottom) in siACTL6A relative to siControl FaDu SCC cells. H3K4me1: enhancer histone mark. H3K4me3: active promoter histone mark. (E) SMARCC1 CUT&RUN peaks across *YAP*, *TAZ*, *TEAD1-4* loci unaltered upon *ACTL6A* knockdown (siACTL6A) compared to control (siControl). (F) RT-qPCR showing relative expression of indicated genes in FaDu SCC cells 48 hours after transfection of *YAP/TAZ* siRNA (siYAP/TAZ) and control siRNA (siControl). Normalized to siControl condition. *$P < 0.05$. n.s.: not significant.

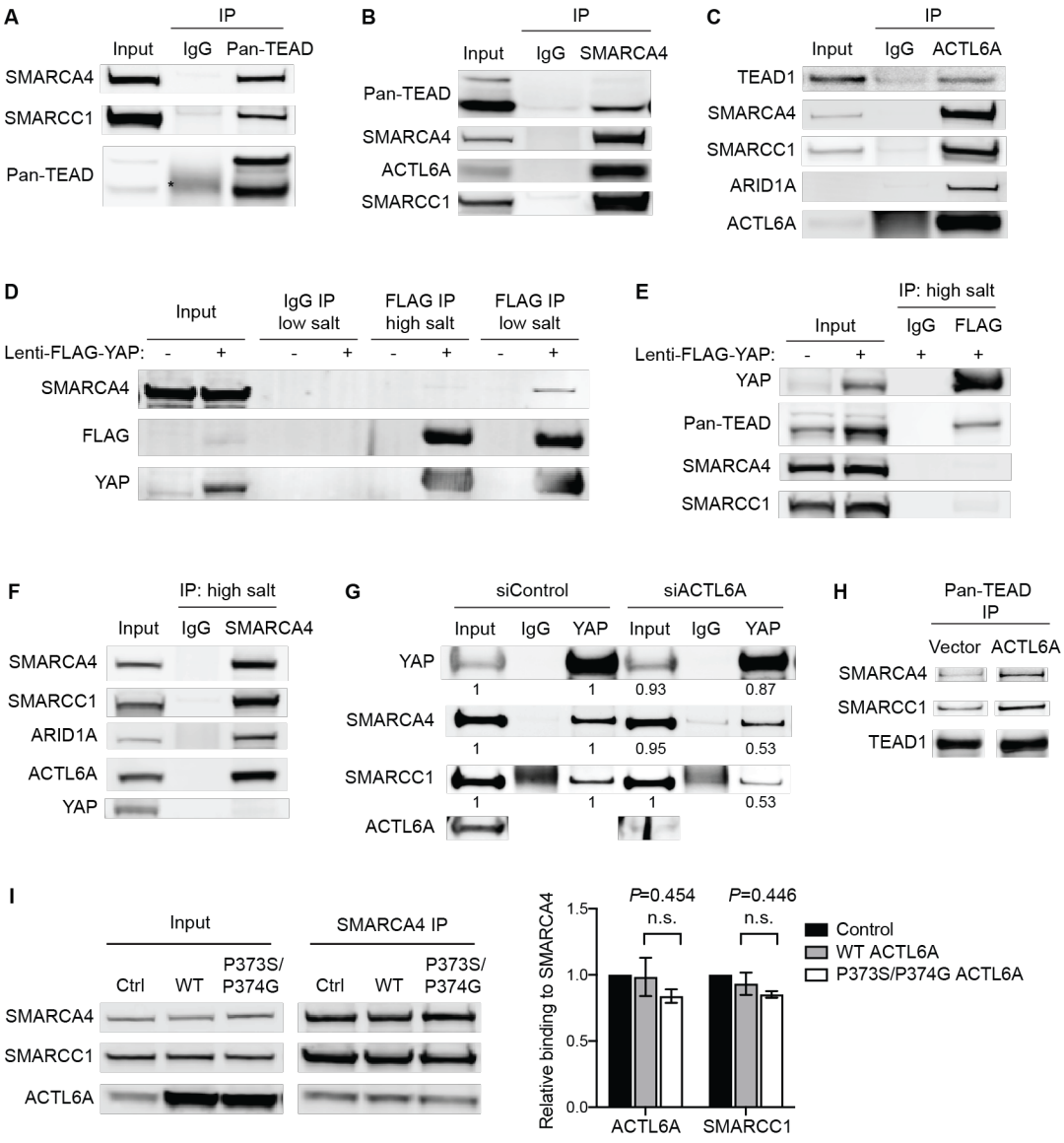

Figure S5. ACTL6A provides surfaces on the BAF complex for TEAD-YAP binding. Related to Figure 5.

(A-C) Co-IP experiments by Pan-TEAD (A), SMARCA4 (B), ACTL6A (C) antibodies with control IgG using nuclear extracts from FaDu SCC cells. *IgG heavy chain. (D) Co-IP experiments by FLAG antibody using nuclear extracts from HEK293T cells transduced by lentivirus expressing FLAG-YAP or empty control. Note the high-salt (500mM) buffer condition abolished the binding between FLAG-YAP and BAF-subunit SMARCA4 and SMARCC1 compared to low-salt (100mM) condition used in (A-C). (E) Purification of FLAG-YAP for the *in vitro* binding assay by FLAG IP under the high-salt condition. Blots showed TEAD proteins were co-precipitated with YAP but not BAF subunits. (F) Purification of BAF complexes for the *in vitro* binding assay by IP using SMARCA4 antibody under the high-salt condition. Blots showed BAF subunits were co-IP'd with SMARCA4 but not YAP. (G) Co-IP by YAP and control IgG antibodies using nuclear extracts from FaDu cells 72 hours after transfection with siACTL6A and siControl. Relative levels normalized to siControl condition. (H) Co-IP experiments by Pan-TEAD antibody in primary human keratinocytes transduced by lentivirus overexpressing *ACTL6A* and the vector control. Note increased binding of BAF subunit SMARCA4 and SMARCC1 to TEAD. Mouse TEAD1 antibody

used for blotting to avoid TEAD signals masked by rabbit Pan-TEAD antibody heavy chain signals. (I) Co-IP by SMARCA4 antibody in nuclear extract from FaDu cells. WT: reconstituting WT ACTL6A into *ACTL6A* CRISPR-KO cells. P373S/P374G: reconstituting P373S/P374G ACTL6A into *ACTL6A* CRISPR-KO cells. Ctrl: lentiviral CRISPR control vector. Quantifications: relative levels of co-IP'd ACTL6A and SMARCC1 in WT and P373S/P374G conditions normalized to ctrl. n=2 experiments. Error bars indicate SEM. n.s.: not significant.

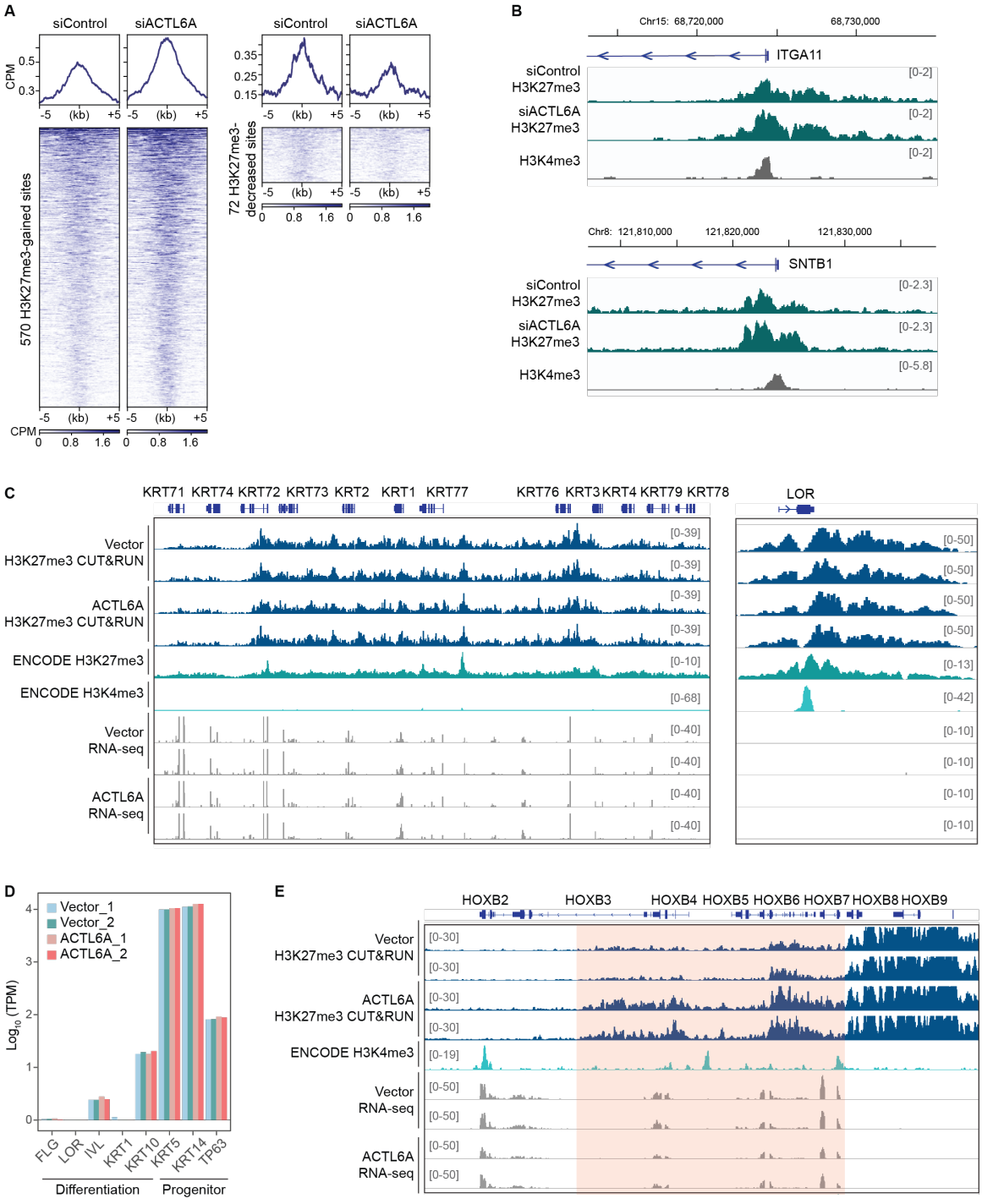
A
siControl
siACTL6A
CPM
570 H3K27me3-gained sites
72 H3K27me3-decreased sites
B
Chr15: 68,720,000
68,730,000
ITGA11
siControl H3K27me3
siACTL6A H3K27me3
H3K4me3
Chr8: 121,810,000
121,820,000
121,830,000
SNTB1
C
KRT71 KRT74 KRT72 KRT73 KRT2 KRT1 KRT77
KRT76 KRT3 KRT4 KRT79 KRT78
LOR
Vector H3K27me3 CUT&RUN
ACTL6A H3K27me3 CUT&RUN
ENCODE H3K27me3
ENCODE H3K4me3
Vector RNA-seq
ACTL6A RNA-seq
D
Vector_1
Vector_2
ACTL6A_1
ACTL6A_2
Log10 (TPM)
FLG
LOR
IVL
KRT1
KRT10
KRT5
KRT14
TP63
Differentiation
Progenitor
E
HOXB2
HOXB3
HOXB4 HOXB5 HOXB6 HOXB7 HOXB8 HOXB9

Figure S6. Genome-wide profiling of H3K27me3 modifications by CUT&RUN identifies regions with altered H3K27me3 domains upon *ACTL6A* knockdown and overexpression. Related to Figure 6.

(A) Heat maps and profiles of H3K27me3 CUT&RUN across H3K27me3-gained (left) and H3K27me3-reduced (right) regions in FaDu SCC cells 72 hours after siACTL6A and siControl transfection. CPM: counts per million. (B) Genome browser tracks of H3K27me3 CUT&RUN upon ACTL6A knockdown. (C) Genome browser tracks of H3K27me3 CUT&RUN and RNA-seq profiles at keratinocyte-differentiation gene *KRT1* and its nearby genes (left), and *LOR* (right) in primary human keratinocytes transduced by lentivirus overexpressing *ACTL6A* and the vector control. Also shown were H3K27me3 and H3K4me3 ChIP-seq tracks in keratinocytes from ENCODE datasets. (D) Expression levels (transcripts per million, TPM) of keratinocyte differentiation genes and progenitor markers between *ACTL6A*-overexpressed and vector-control keratinocytes. (E) Genome browser tracks as in (A) at the *HOXB* locus.

SUPPLEMENTAL TABLES

Table S1. qPCR primers used in this study. Related to Figures 3.

Gene (human)	Forward primer	Reverse primer
ACTL6A	AGTGGCAGGAGGAAACACAC	CCCAAAGAGGCTAGAATGGA
YAP	GCACCTCTGTGTTTTAAGGGTCT	CAACTTTTGCCCTCCTCCAA
TAZ	GGCTGGGAGATGACCTTCAC	CTGAGTGGGGTGGTTCTGCT
PPIB	CGTCTTCTTCCTGCTGCTG	AGCCAAATCCTTTCTCTCCTG
WWC1	TCTACCAGGTGAAGCAGCAG	GCTGGATGATGAACCAGAGAC
CTGF	AGGAGTGGGTGTGTGACGA	CCAGGCAGTTGGCTCTAATC
AXL	CACCAGCAAGAGCGATGTGT	CGGTCCTGGGGATTTAGCTC
OLR1	TTGCCTGGGATTAGTAGTGACC	GCTTGCTCTTGTGTTAGGAGGT
TGM2	GGCACCAAGTACCTGCTCA	AGAGGATGCAAAGAGGAACG
BRPF3	GGAAGGTGTGAACGGAGACT	GTCTCCGCGGTCTTCAAA
CAVIN2	GGCAGGTATGACAGCTTACGG	GTTGTCCACCGGCTGTAATGT
IGFBP3	AGAGCACAGATACCCAGAACT	GGTGATTCAGTGTGTCTTCCATT
FNDC3B	GAGCATGCTGCATCAGTACC	GTGCGAACAGGGAGACTTTC
TYRO3	GAGAGGAACTACGAAGATCGGG	AGTGCTTGAAGGTGAACAGTG
CNN3	GGCAGGTATGACAGCTTACGG	GTTGTCCACCGGCTGTAATGT